

# An engineer's approach: How can 10-100 $\mu\text{T}$ , 10-100 Hz magnetic field influence human cardiovascular regulation?

J.J. Niederhauser<sup>1</sup>

<sup>1</sup>InnoClever GmbH, Tiergartenstrasse 7, 4410 Liestal, Switzerland  
Contact: joel.niederhauser@innoclever.com

## Introduction

In 1896 Arsène d'Arsonval reported symptoms of altered cardiovascular regulation in subjects plunging the head into a 42 Hz magnetic field (MF) in the order of 100  $\mu\text{T}$  in a large solenoid [1]. He also reported magnetophosphenes induced by magnetic field of a smaller coil.

Magnetophosphenes have been extensively studied and a frequency dependent threshold in the order of 5-10 mT MF at the retina has been established [2].

The influence of MF on cardiovascular regulation has received less attention. Studies below 1  $\mu\text{T}$  and above 100  $\mu\text{T}$  reported no effect. As shown in Figure 1 there are repeated reports in the 10-100  $\mu\text{T}$  exposure range, especially when challenging the sympathetic part of cardiovascular regulation, that showed influence of 16-60 Hz MF on slowing heart rate and altered heart rate variability in human subjects [1–21].

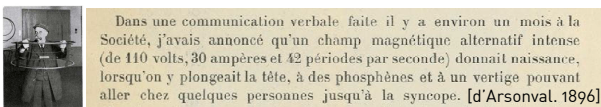
We approach the topic from an engineering perspective and present a putative mechanism for influence of 10-100  $\mu\text{T}$ , 10-100 Hz magnetic field on human cardiovascular regulation.

of the mechanoreceptors shows no firing below a threshold (e.g. 80 mmHg) and pressure dependent firing rate above the threshold.

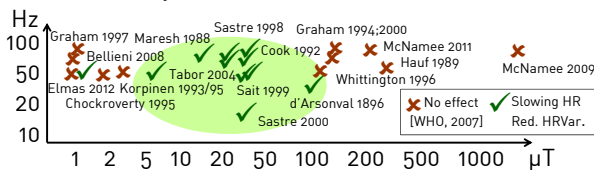
The baroreceptor signal is processed in the nucleus of the solitary tract in the brainstem. Depending on systolic (e.g. 120 mmHg) and diastolic (e.g. 80 mmHg) pressure, there are two distinct feedback mechanisms: (1) parasympathetic autonomous control slows heart rate if systolic pressure is too high, (2) sympathetic autonomous control increases blood vessel constriction and slightly increases heart rate if diastolic pressure is too low. The sympathetic effect on low frequency heart rate fluctuation is an order of magnitude below the parasympathetic effect.

This work has focus on the sympathetic autonomous control mechanism operating at noise level of the baroreceptors. The sympathetic system resembles a discrete-time signal processing design clocked at the heart beat. The output generates sympathetic bursts. For each heartbeat there either is a sympathetic burst or there is no sympathetic burst. The probability of having a sympathetic burst depends on the diastolic pressure level. There is a 1.4 second latency between the sampling of the diastolic pressure and the corresponding generated output sympathetic burst. Increased muscular sympathetic nerve activity (MSNA) results in increased blood vessel constriction by direct nerve path and indirectly by the renin-angiotensin hormone system.

### 120 years since Arsène d'Arsonval's observation ✓



### Soviet switchyard worker studies [Marino et al., 1977] ✓



### MF exposure studies with slowing heart rate effect ✓

**Figure 1:** Studies showing influence of magnetic field on human cardiovascular regulation.

## Materials and Methods

### Anatomy and physiology analysis

From an engineering perspective human cardiovascular regulation can be seen as a non-linear closed loop control system aiming at stabilizing blood pressure and oxygen supply to the human brain.

Baroreceptors in the carotid arteries (neck) are sensors for blood pressure and flow. The pressure dependent firing rate

### Baroreceptor signal encoding

From engineering perspective the pressure dependent baroreceptor signal output used two encodings. Systolic pressure is encoded using frequency modulation (FM) and diastolic pressure is encoded using pulse width modulation (PWM). The PWM duty cycle is lower for reduced diastolic pressure because of the longer silence period corresponding to pressure level below the baroreceptor firing threshold.

External interference at or above the noise level may shorten the silence period resulting in a PWM encoded pressure signal reading that appears to be higher than the actual diastolic pressure. This may influence the sympathetic control and result in widening of blood vessels, slightly slowing heart rate and reduced oxygen supply to the human brain.

### Magnetic field and firing probability

Time varying magnetic field induces electric field and currents in human body and electric field across excitable

cell membranes (e.g. carotid baroreceptor sensory cells). This time-coherent firing probability modulation is averaged over surface of each cell and across all sensory cells in a converging neural network (see Fig. 2). Signal (magnetic field modulated firing probability) to noise ratio is increased by coherent averaging.

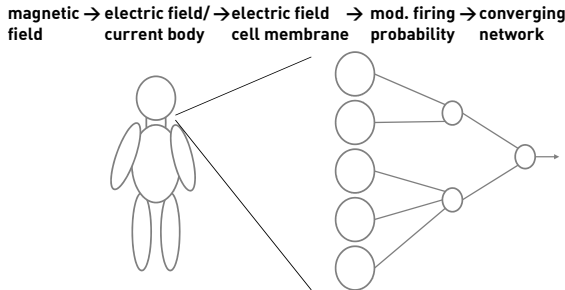


**Figure 2:** Time varying magnetic field induces electric field and currents in human body resulting in electric field across excitable cell membranes. Firing probability is coherently modulated and averaged over sensor surface and converging neural network.

### Sensor noise level

The noise level of a sensor scales with  $\sqrt{n}$  for  $n$  times spatial or temporal averaging.

The human visual system can not only detect light but also magnetic field (magnetophosphenes) and pressure (pressure phosphenes). Assuming similar technology, the MF threshold of the baroreceptors may be calculated from the well established visual system magnetophosphene threshold using the temporal (bandwidth) and spatial (area) averaging properties of the two sensors.

The peripheral retina has a rod density of  $40'000/\text{mm}^2$ . With 1000 converging rods the sensor area is  $1/40 \text{ mm}^2 = 0.025 \text{ mm}^2$ . The bandwidth of the visual system is 40 Hz and the MF noise-level is 5-10 mT (magnetophosphene threshold).

Carotid arteries with a diameter of 5 mm have 15.7 mm circumference. Assuming 10 mm length the baroreceptor sensor area can be estimated to be  $157 \text{ mm}^2$ . The bandwidth of the sensor is in the order of 1 Hz.

Compared with retina sensors the baroreceptor sensors have relative spatial averaging  $n_{area} = 157/0.025 = 6283$  and relative temporal averaging  $n_{bandwidth} = 40/1 = 40$ .

### Simple converging sensory neuron network model

We propose a simple converging sensory neural network model with following properties. Non-linear, discrete-time simulation at 1 ms resolution. 1000 input firing signals with modulated firing probability density function (pdf) and 3 stage 10:1 converging coincident detection. The model corresponds to feed-forward converging network path from firing probability modulation in sensory cells to cardiovascular regulation system in the brainstem. The number input

cells was chosen in the order of magnitude of fibre numbers in sensory nerves and visual rods networks. The three stage design is an assumption and is not based on anatomic knowledge. The fundamental behaviour, however, is not expected to depend on a specific number of stages.

The MATLAB code of the model:

```
% Simple converging sensory neural network
%
% Joel Niederhauser, July 2017
%
% This simple model simulates 1000 random firing units converging into
% 100, 10, 1 output signal using 1 ms resolution discrete time model

n=1000; % generate 1000 units
t=20; % simulation period in ms (50 Hz)
stages = 3; % 3 converging stages
thr = 2; % threshold for 3 stages

res=[]; % result
res_f=[]; % modulation factor for result

graph=0; % show graph (0 = no intermediate graphs, 1 = show graphs)
range = -2:0.01:3; % calculate
% f = 3; range=log10(f); graph=1; % produce graphs for factor 3
% f = 100; range=log10(f); graph=1; % produce graphs for factor 100

for e=range;

f = 10.^e % logarithmic scaling

pn = (ones(t,1)-f*cos(2*pi*(1:t)'/t))*1/40; % cos modulated PDF

pn(pn<0)=0; % limit probability density function to 0..1
pn(pn>1)=1;

pn_sum=cumsum(pn); % cumulative distribution function
pn_sum(pn_sum<0)=0; % limit cdf to 0..1
pn_sum(pn_sum>1)=1;

if graph
figure(1); plot(pn); axis([-inf inf 0 1]); title(['probability density function'
num2str(f)]);
figure(2); plot(pn_sum); axis([-inf inf 0 1]); title(['cumulative distribution
function' num2str(f)]);
end

r=rand(n,1); % generate 1000 random firing probabilities

un=zeros(n,1); % prepare firing time

for i=1:n % calculate firing time for each sensory neuron
ind=find(pn_sum<=r(i));
if (isempty(ind))
un(i)=0;
else
un(i)=ind(end);
end
end

if graph
figure(3); hist(un,0:19); % histogram of all firing events
end

% converge network
ma = zeros(t+1,n); % prepare firing matrix
ma((1:t+1:n*(t+1))'+un) = 1;% firing event for 1000 neurons
ma(end,:)=[]; % ignore all neurons that did not fire
if graph
figure(4); imagesc(ma'); title(['stage 0: 1000 neuron firing f=' num2str(f)]);
end;
ma2 = zeros(t,n/10);
for i=1:100 % converge 1000->100 neurons
ma2(:,i) = sum(ma(:,(1:10)+(i-1)*10),2); % sum firing coincidents
end

if graph
figure(5); imagesc(ma2'); title(['stage 1: 100 neuron coincidents' num2str(f)]);
end

ma3=ma2>=thr; % two or more coincident firings at input?

if graph
figure(6); imagesc(ma3'); title(['stage 1: 100 neuron firing' num2str(f)]);
end;

ma4 = zeros(t,n/100);
for i=1:10 % converge 100->10 neurons
ma4(:,i) = sum(ma3(:,(1:10)+(i-1)*10),2);
end
if graph
figure(7); imagesc(ma4'); title(['stage 2: 10 neuron coincidents' num2str(f)]);
end;

ma5=ma4>=thr; % two or more coincident firings at input?
if graph
figure(8); imagesc(ma5'); title(['stage 2: 10 neuron firing' num2str(f)]);
end

ma6 = zeros(t,n/1000);
for i=1:1 % converge 10->1 neuron
ma6(:,i) = sum(ma5(:,(1:10)+(i-1)*10),2);
end

if graph
figure(9); imagesc(ma6'); title(['stage 3: 1 neuron coincidents' num2str(f)]);
end;
```



```

ma7=ma6>thr; % two or more coincident firings at input?
if graph
figure(10); imagesc(ma7'); title(['stage 3: 1 neuron firing' num2str(f)]);
end;
res=[res;sum(ma7)]; % store total firing counts as result
res_f=[res_f;f]; % store factor as result parameter
end;
figure(100);semilogx(res_f,res,'linewidth',2);
title('Simple converging network model 3 stages');
ylabel('firing rate [a.u.]');
xlabel('modulation factor');

```

## Results

### Sensor sensitivity threshold

The noise level of a sensor scales with  $\sqrt{n}$  for  $n$  times spatial or temporal averaging. The MF threshold is expected to scale with  $1/\sqrt{n} = 1/\sqrt{n_{area} \cdot n_{bandwidth}} = 1/\sqrt{6283 \cdot 40} = 1/500$ .

Based on the magnetophosphenes threshold of 5-10 mT the MF threshold for baroreceptor sensor can be calculated to be at 5-10 mT / 500 = 10-20  $\mu$ T.

This threshold is in the same order of magnitude as previously estimated theoretical limit for human sensitivity to weak fields [2, 22].

### Simple converging sensory neural network model

The output of the MATLAB simulation is shown in Fig. 3 and 4. For modulation below the sensitivity threshold there are only one or two firing events at the output of the converging network. For modulation factor 3 the firing rises up to 8 or 9 events. For larger modulation the number of firing events decreases to one or two.

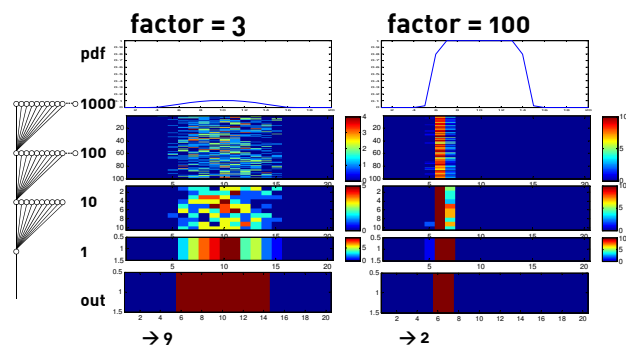


**Figure 3:** Result for two modulation factors: modulated probability density function (pdf) and coincident detection for each stage of the simple model. Factor 3 generates 9 firing events. Factor 100 generates only 2 firing events at the output.

## Discussion

The MF sensitivity threshold of the baroreceptor sensors was calculated from the known phosphene threshold using simple geometry and bandwidth considerations. The result of 10-20  $\mu$ T is in the same order of magnitude as previous theoretical human sensitivity threshold estimation [2, 22].

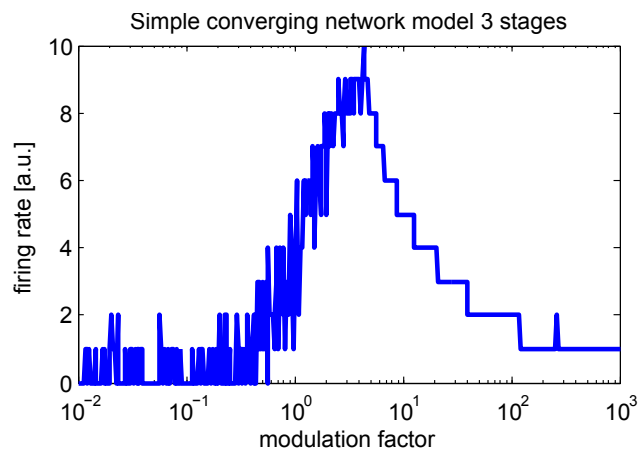


**Figure 4:** Result of simple converging neural network model for modulation factor range showing amplitude window effect.

The MF field may interfere with the silent period of the baroreceptor diastolic pressure measurement influencing the correct regulation of the blood vessel constriction. If the sympathetic regulation is influenced or inhibited by MF interference a change in dynamic control behaviour may be observed when properly challenged (e.g. changing ambient temperature or drawing blood).

The simple converging neural network may provide an explanation why influence of MF on cardiovascular regulation was reported at 10-100  $\mu$ T in human studies [1–21] but not observed in studies with higher MF.

Acute cardiovascular effects may reduce cerebral oxygen supply and should be considered in safety regulations.

## Conclusions

Based on phosphene threshold we estimate a magnetic field sensitivity threshold for baroreceptor and cardiovascular regulation in the 10-20  $\mu$ T range.

A simple converging neural network model demonstrates amplitude window behaviour as possible explanation for lack of observed human cardiovascular effect in higher magnetic field exposure studies.

## References

- [1] Arsène d'Arsonval. Dispositifs pour la mesure des courants alternatifs de toutes fréquences. In *Comptes rendus des séances de la Société de biologie et de ses filiales*, volume 48, pages 450–451. Société de biologie (Paris, France), 1896.
- [2] World Health Organization et al. Extremely low frequency fields. 2007.
- [3] Andrew A Marino and Robert O Becker. Biological effects of extremely low frequency electric and magnetic fields: a review. *Physiol Chem Phys*, 9(2):131–147, 1977.
- [4] CM Maresh, MR Cook, HD Cohen, C Graham, and WS Gunn. Exercise testing in the evaluation of human responses to powerline frequency fields. *Aviation, space, and environmental medicine*, 59(12):1139–1145, 1988.



- [5] Mary R Cook, Charles Graham, Harvey D Cohen, and Mary M Gerkovich. A replication study of human exposure to 60-hz fields: Effects on neurobehavioral measures. *Bioelectromagnetics*, 13(4):261–285, 1992.
- [6] L Korpinen, J Partanen, and A Uusitalo. Influence of 50 hz electric and magnetic fields on the human heart. *Bioelectromagnetics*, 14(4):329–340, 1993.
- [7] L Korpinen and J Partanen. The influence of 50 hz electric and magnetic fields on the extrasystoles of human heart. *Reviews on environmental health*, 10(2):105–112, 1994.
- [8] Charles Graham, Mary R Cook, Harvey D Cohen, and Mary M Gerkovich. Dose response study of human exposure to 60 hz electric and magnetic fields. *Bioelectromagnetics*, 15(5):447–463, 1994.
- [9] Charles Graham, Mary R Cook, Donald W Riffle, Mary M Gerkovich, and Harvey D Cohen. Nocturnal melatonin levels in human volunteers exposed to intermittent 60 hz magnetic fields. *Bioelectromagnetics*, 17(4):263–273, 1996.
- [10] Charles Graham, Mary R Cook, Donald W Riffle, MM Gerkovich, and HD Cohen. Human melatonin during continuous magnetic field exposure. *Bioelectromagnetics*, 18(2):166–171, 1997.
- [11] Charles Graham, Mary R Cook, Robert Kavet, Antonio Sastre, and Deborah K Smith. Prediction of nocturnal plasma melatonin from morning urinary measures. *Journal of pineal research*, 24(4):230–238, 1998.
- [12] Antonio Sastre, Mary R Cook, and Charles Graham. Nocturnal exposure to intermittent 60 hz magnetic fields alters human cardiac rhythm. *Bioelectromagnetics*, 19(2):98–106, 1998.
- [13] Mardi L Sait, Andrew W Wood, and Hassan A Sadafi. A study of heart rate and heart rate variability in human subjects exposed to occupational levels of 50 hz circularly polarised magnetic fields. *Medical Engineering and Physics*, 21(5):361–369, 1999.
- [14] Mardi L Sait, Andrew W Wood, and Hassan A Sadafi. Human heart rate changes in response to 50 hz sinusoidal and square waveform magnetic fields: a follow up study. In *Electricity and Magnetism in Biology and Medicine*, pages 517–520. Springer, 1999.
- [15] Charles Graham, Mary R Cook, Antonio Sastre, Mary M Gerkovich, and Robert Kavet. Cardiac autonomic control mechanisms in power-frequency magnetic fields: a multistudy analysis. *Environmental health perspectives*, 108(8):737, 2000.
- [16] Zbysław Tabor, Jozef Michalski, and Eugeniusz Rokita. Influence of 50 hz magnetic field on human heart rate variability: Linear and nonlinear analysis. *Bioelectromagnetics*, 25(6):474–480, 2004.
- [17] Emilio Baldi, Claudio Baldi, and Brian J Lithgow. A pilot investigation of the effect of extremely low frequency pulsed electromagnetic fields on humans' heart rate variability. *Bioelectromagnetics*, 28(1):64–68, 2007.
- [18] Simone Rossi, Mark Hallett, Paolo M Rossini, and Alvaro Pascual-Leone. Safety, ethical considerations, and application guidelines for the use of transcranial magnetic stimulation in clinical practice and research. *Clinical neurophysiology*, 120(12):2008–2039, 2009.
- [19] Narcis Iulian Adochiei, Georg Dorffner, and Valeriu David. Heart rate variability monitoring due to 50 hz electromagnetic field exposure and statistical processing. In *Electrical and Power Engineering (EPE), 2012 International Conference and Exposition on*, pages 610–613. IEEE, 2012.
- [20] Joël Niederhauser, Roman Schmied, Mathias Baudenbacher, Christian Schindler, Brian Litt, and Martin Rössli. Magnetic field triggered syncope – from jaques-arsène d'arsoval's first observation in 1896 to car accident injury statistics after power-line motorway crossings in switzerland. In *BioEM2015 conference*, number PA-39, pages 223–227. Bioelectromagnetics Society, jun 2015.
- [21] Joël Niederhauser, Roman Schmied, Mathias Baudenbacher, Christian Schindler, and Martin Rössli. Influence of power-transmission-lines on car accidents. In *BioEM2016 conference*, number PA-213, pages 564–569. Bioelectromagnetics Society, jun 2016.
- [22] Robert K Adair, R Dean Astumian, and James C Weaver. Detection of weak electric fields by sharks, rays, and skates. *Chaos: An Interdisciplinary Journal of Nonlinear Science*, 8(3):576–587, 1998.

## Acknowledgments

The author thanks A. Legros and S. Villard from the Lawson Institute in London, Canada for discussion and for the possibility to see the magnetophosphenes in their MF exposure facility. The author acknowledges the support of A. Wood and his group from Swinburne University in Melbourne, Australia for the introduction to their MF exposure lab and and discussion of their blinded human heart-rate studies.